Materials Science & Engineering A 717 (2018) 113–123

Contents lists available at ScienceDirect

Materials Science & Engineering A

journal homepage: www.elsevier.com/locate/msea

The influence of Sc solute partitioning on ductile fracture of Sc-microalloyed Al-Cu alloys

C. Yang, D. Shao, P. Zhang, Y.H. Gao, J.Y. Zhang, J. Kuang, K. Wu, G. Liu*, J. Sun*

State Key Laboratory for Mechanical Behavior of Materials, Xi'an Jiaotong University, Xi'an 710049, China

ARTICLE INFO

Keywords:
Aluminum alloys
Microalloying effect
Interfacial segregation
Solute partitioning
Ductile fracture

ABSTRACT

Al-XCu (X = 1.0, 1.5, and 2.5 wt%) alloys with and without 0.3 wt% Sc addition were prepared respectively. The effects of composition and heat treatment processes on the microstructural evolution were systematically investigated by using transmission electron microscope and atom probe tomography (APT). Both Al_3Sc dispersoids and θ'-Al_2Cu precipitates coexisted after artificial aging, and a strong Sc segregation at θ'-Al_2Cu/matrix interfaces was detected and quantified through APT examinations. A Sc solute partitioning was demonstrated between in the Al_3Sc dispersoids and at the θ'-Al_2Cu/matrix interfaces, mediated by the Cu content. Increasing the Cu content, both the size and volume fraction of the Al_3Sc decreased after solid solution treatment. As a result, the interfacial Sc segregation was accordingly intensified during subsequent aging treatment. A parameter of reduction in interfacial energy ($\Delta\gamma$), derived from APT analyses, was proposed to characterize the degree of interfacial Sc segregation. The coupling effect of Al_3Sc dispersoids and θ'-Al_2Cu precipitates on ductile fracture was discussed, where a micromechanical model was developed to describe a quantitative relationship between the fracture strain with $\Delta\gamma$ as well as parameters of the Al_3Sc dispersoids.

1. Introduction

Aluminum alloys have attracted increasing attentions because of their low density, high stiffness and good strength. As an important kind of structural materials, heat-treatable aluminum alloys have been extensively applied in aircraft and automobiles. Unfortunately, the ductility of metals generally decreases as the strength is raised by alloying and heat treatment. In order to obtain excellent mechanical properties for heat-treatable aluminum alloys, extensive studies [1–7] have been carried out to understand the trade-off between strength and ductility in heat-treated aluminum alloys, where second phase particles play important roles. Usually, three classes of second phase particles are present in the heat-treatable aluminum alloys, i.e., coarse constituents, intermediate dispersoids and fine precipitates. It is now broadly known that: (i) under service loading, the coarse constituents in micrometers size are primary void initiators or preferential crack propagating path; (ii) decohesion of the dispersoids in sub-micrometer size will form void sheets and hence accelerate void growth; (iii) the fine precipitates can strengthen the alloys by pinning the moving dislocations, which, however, will cause the local strain/stress concentration and degrade the deformation capability. In addition, the three classes of second phase particles generally affect the ductile fracture in coupling [2,8,9].

Microalloying is an effective way to improve the performance of aluminum alloys. Trace additions of microalloying elements are of prime importance in modifying the precipitation/micro-structure and improving the mechanical properties of Al alloys [10]. For example, additions of minor Cd, In and Sn increase both the rate and extent of hardening in Al–Cu alloys, because these elements suppress the formation of the GP zones and the θ''-Al_2Cu and stimulate a finer and more uniform dispersion of the θ'-Al_2Cu [11]. Two mechanisms have been proposed: one is that the microalloying elements segregate at the precipitate/matrix interface, resulting in a reduction of the interfacial energy [11–13] , the other is that the trace elements facilitate heterogeneous nucleation directly at Sn (Cd or In)-rich particles [14,15]. Another example is that [16–21] minor additions of Sc and Zr in Al alloys can significantly increase the strength and prevent the recrystallization by forming $Al_3(Sc_XZr_{1-x})$ dispersoids and precipitates during heat treatment. Recently, some of present authors [22,23] showed that addition of trace amounts of Sc in Al–Cu alloys remarkably inhibited the θ'-Al_2Cu precipitate growth and promoted the homogeneous θ'-Al_2Cu precipitation by the Sc segregation at the θ' precipitate/matrix interface, while highly coarsening-resistant Al_3Sc dispersoids were formed additionally. They focused mainly on the θ'-Al_2Cu precipitate strengthening affected by the interfacial Sc segregation and the θ'-Al_2Cu precipitate influence on the ductile fracture. However, the Al_3Sc dispersoids were not considered in analyzing the ductile fracture.

* Corresponding authors.
E-mail addresses: lgsammer@mail.xjtu.edu.cn (G. Liu), junsun@mail.xjtu.edu.cn (J. Sun).

https://doi.org/10.1016/j.msea.2018.01.078
Received 3 November 2017; Received in revised form 2 January 2018; Accepted 20 January 2018
0921-5093/

Nomenclature

$\bar{r}_d^h$	The average radius of Al_3Sc after homogenization treatment
N_d^h	The number density of Al_3Sc after homogenization treatment
$\bar{r}_d^s$	The average radius of Al_3Sc after solution treatment
f_d^s	The volume fraction of Al_3Sc after solution treatment
λ_d^s	The interparticle spacing of the Al_3Sc dispersoids
$\bar{r}_p$	The average radius of Al_2Cu after aging treatment.
N_p	The number density of Al_3Sc after aging treatment
λ_p	The interparticle spacing of the Al_2Cu precipitates
r_d^{cri}	The critical size for coherent to semi-coherent transition of the Al_3Sc dispersoids during homogenization treatment
γ	The interfacial free energy
γ_{CI}	The interfacial free energy for coherent interfaces
γ_{SCI}	The interfacial free energy for the semi-coherent interfaces
$\Delta\gamma$	The reduction in interfacial free energy
$\Delta\gamma_{CI}$	The reduction in interfacial free energy for the coherent interfaces
$\Delta\gamma_{SCI}$	The reduction in interfacial free energy for the semi-coherent interfaces

Actually, the formation of Al_3Sc dispersoids during homogenization and their evolution during solid solution manipulate the Sc atoms available for the interfacial segregation at the θ'-Al_2Cu/matrix interfaces during aging treatment. This means that a Sc partitioning should exist between in the Al_3Sc dispersoids and at the θ'-Al_2Cu/matrix interfaces. What factors may impact this Sc partitioning and how the partitioning affects the ductile fracture of the alloys are far from clear. Further studies are in urgent need to optimize the microstructure and enhence the mechanical properties.

In this paper , Al-Cu-Sc alloys with different Cu contents but a constant Sc addition are studied for comparison. The Cu-dependent Al_3Sc dispersoids evolution and concomitantly the Sc segregation-related θ'-Al_2Cu precipitation will be concerned. The coupling effect of Al_3Sc dispersoids and θ'-Al_2Cu precipitates on the ductile fracture, mediated by the Cu content, will be in particular investigated.

2. Experimental procedures

2.1. Material preparation and heat treatments

Alloys with compositions of Al-X wt% Cu alloys (X = 1.0, 1.5, and 2.5, abbreviated Al-XCu alloys), Al-X wt% Cu-0.3 wt% Sc alloys (Al-XCu-Sc), and Al-0.3 wt% Sc alloy (Al-Sc) were melted and cast in an argon stream; 99.99 wt% pure Al, 99.99 wt% pure Cu, and Al-2.0 wt% Sc master alloy were used. The cast ingots were homogenized at 723 K for 5 h. All the alloys were subsequently solutionized at 853 K for 3 h and terminated by water quenching to room temperature, aging was performed in air at 523 K for 8 h. The maximum error of all temperature measurements in the present experiments was ± 1 K. Fig. 1 illustrates the process of heat treatment.

2.2. Microstructural characterizations

Microstructures of the alloys were characterized by using transmission electron microscopy (TEM) and high-resolution TEM (HRTEM). TEM was carried out using a JEOL 2100F operating at 200 kV. Quantitative evaluations of the number density and size of the second phase particles (Al_3Sc dispersoids and θ'-Al_2Cu precipitate) were reported as average values of more than 300 measurements. The volume fraction of the second phase particles was determined by employing a corrected projection method [2,24], in which the foil thickness of each captured region was obtained through convergent beam electron diffraction patterns [25]. Using the raw radius data of particles and the foil thickness in each area, the radius distributions were calculated after correction for the truncation effects based on a method by Crompton *et al.* [26]. Details about the measurements can be referred to previous publications [2,22,23,27–29].

To visibly reveal the microalloying mechanism at the atomic level, atom probe tomography (APT) was performed using an Imago Scientific Instruments 3000HR local electrode atom probe (LEAP). APT sample blanks with a square cross-sectional area of approximately 0.3 × 0.3 mm^2 and a length of 1 cm were prepared by a combination of slicing and mechanical grinding. A two-step electropolishing procedure was used for making tips from these blanks [30,31]. A 10 vol% perchloric acid in methanol solution was used for coarse polishing, and the final polishing was performed using a solution of 2 vol% perchloric acid in butoxyethanol. APT data collection using the electrical pulsing mode was performed at a specimen temperature of 30 ± 0.3 K, with a voltage pulse fraction (pulse voltage/steady-state DC voltage) of 20%, a pulse repetition rate of 200 kHz and a background gauge pressure of $< 6.7 \times 10^{-8}$ Pa (5×10^{-10} Torr).

2.3. Measurements of mechanical properties at RT

Tensile testing at room temperature was used to measure room temperature yield strength (σ_0) and strain to fracture (ε_f) of the samples after artificial aging treatment. The smooth dog-bone-shaped tensile specimens have a gauge size of 6 *mm* in diameter and 30 *mm* in length. The testing was performed at a constant strain rate of 5×10^{-4} s^{-1} with the load direction parallel to the specimen axis. The yield strength was determined as the 0.2% offset, and the strain to fracture was determined as $\varepsilon_f = \ln(A_o/A_f)$, where A_o is the initial area and A_f is the area at fracture of the specimens.

3. Results

Fig. 2 representatively shows optical images of the Al-2.5Cu and Al-2.5Cu-Sc alloys for comparison. Measurements show that the Al-XCu alloys have equiaxed grains with average size of 1.0 – 2.0 mm, and the grain size of the Al-XCu-Sc alloy (0.3 – 0.6 mm) is significantly smaller than that of the Al-XCu alloys (quantitatively see Table 1). It has been reported that small amounts of scandium adding in Al alloys may lead to the formation of Al_3Sc particles. The presence of Al_3Sc particles can

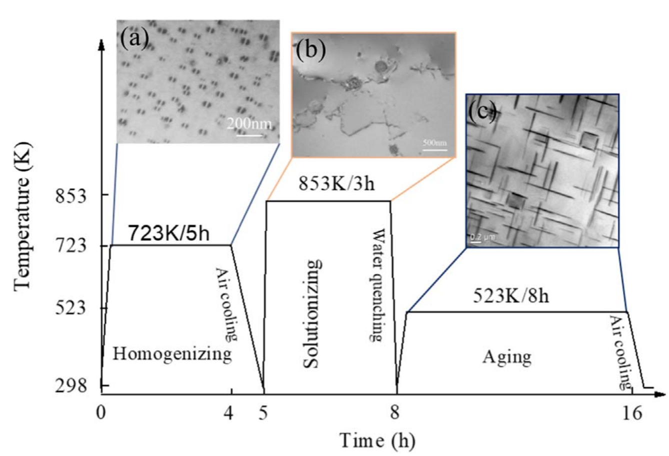

Fig. 1. A schematic diagram illustrating the heat treatments and involved microstructural evolution.